RSC Advances

ROYAL SOCIETY OF CHEMISTRY

www.rsc.org/advances

Exchange of cysteamine, thiol ligand in binuclear cationic tetranitrosyl iron complex, for glutathione

L.A. Syrtsova, N.A. Sanina, E.N. Kabachkov, N.I. Shkondina, A.I. Kotelnikov, S.M. Aldoshin

L.A. Syrtsova () N.I. Shkondina A. I. Kotelnikov

Department of kinetics of chemical and biological processes, Institute of Problems of Chemical Physics of the Russian Academy of Sciences, 1, Acad. Semenov av, 142432 Chernogolovka, Moscow Region, Russian Federation.

Fax: +7 (496) 5223507 E-mail-address: syrtsova@icp.ac.ru

N.A. Sanina S.M. Aldoshin

Department of structure of matter, Institute of Problems of Chemical Physics of the Russian Academy of Sciences, 1, Acad. Semenov av, 142432 Chernogolovka, Moscow Region, Russian Federation

E.N. Kabachkov

Department of functional inorganic materials, Institute of Problems of Chemical Physics of the Russian Academy of Sciences, 1, Acad. Semenov av, 142432 Chernogolovka, Moscow Region, Russian Federation

Abstract

This paper describes the comparative study of the decomposition of two iron nitrosyl complexes (NICs) with a cysteamine thiolate ligands $\{Fe_2[S(CH_2)_2NH_3]_2(NO)_4\}SO_4 \cdot 2.5H_2O$ ***(I)*** and a glutathione (GSH)-ligands, $[Fe_2(SC_{10}H_{17}N_3O_6)_2(NO)_4]SO_4 \cdot 2H_2O$ ***(II)***, which spontaneously evolve NO in aqueous medium. NO formation was measured by using spectrophotometric method by the formation of a hemoglobin (Hb)-NO complex. Spectrophotometry and mass-spectrometry methods have firmly shown that the cysteamine ligands are exchanged for 2 GS^- during decomposition of $1.5 \cdot 10^{-4}$ M ***(I)*** in the presence of 10^{-3} M GSH, with 77 % yield at 68 h. As has been established, such behaviour is caused by the resistance of ***(II)*** to decomposition due to the higher affinity of iron to GSH in the complex. The discovered reaction may impede S-

glutathionation of the essential enzyme systems the presence of ***(I)*** and is important for metabolism of NICs, connected with their anti-tumor activity.

Keywords biomedicine iron-sulfur-cluster ligand binding mass spectrometry nitric oxide heme

Abbreviations

(I) complex $\{Fe_2[S(CH_2)_2NH_3]_2(NO)_4\}SO_4 \cdot 2.5H_2O$

(II) complex $[Fe_2(SC_{10}H_{17}N_3O_6)_2(NO)_4]SO_4 \cdot 2H_2O$

NIC nitrosyl iron complex

GSH glutathione

GS-SG oxidized glutathione

1. Introduction

Non-heme nitrosyl iron complexes (NICs) with functional sulfur-containing ligands are of great interest for medical studies due to their biological and pharmacological activity [1-5]. These complexes belong to a new class of efficient exogenous donors of nitric oxide (NO), an important bioregulatory agent for various physiological processes [6-11].***(I)*** is an inducer of apoptosis in human leukemia erythroblastic cells (line K562) and human colon carcinoma (line LS174T) [12]. Investigation of mechanisms of nitrosyl iron complexes activity and their transformation in solutions is particularly important for NO therapy. We have chosen reduced glutathione (GSH) to study ligand exchange reactions with ***(I).*** GSH is a water-soluble tripeptide consisting of amino acids – glutamic acid, cysteine and glycine. GSH is the most commonly encountered non-protein thiol in animal, and its concentration in human tissues varies from 0.1 to 10 mM. The highest concentration is found in the liver, spleen, kidneys, crystalline lens, erythrocytes and leucocytes. The functions of GSH are vital and versatile. Its cysteine thiol acts as a nucleophile in reactions with endogenous and exogenous compounds. Its main functions are 1) antioxidant, 2) co-factor of numerous cytoplasmic enzymes and 3) thiolating agent at significant post-translation modification of a number of cellular proteins. The correlation between metabolism of GSH and such diseases such as cancer, neurodegenerative diseases, cystic fibrosis, HIV and aging [13] has been established. Moreover GSH may promote S-

glutathionation of essential enzymes, receptors, structural proteins, transcription factors and transport proteins [14]. Ligand-glutathione exchange reaction is very important for anti-tumor activity of the complex by causing its bifunctionality, i.e., in addition to the NO donating activity, this complex binds glutathione thus preventing S-S-glutathionation of essential enzyme systems and giving back the anti-tumor activity to them [14]. Therefore it is crucial to understand whether this reaction is common for nitrosyl iron complexes with functional sulfur containing ligands, in particular, for complexes with cationic structure.

Materials and methods

Materials

We used bovine Hb, Tris (Serva, Germany), acetonitrile LC-MS grade (Panreac, Spain), reduced L-glutathione, KI (ALDRICH, USA), $Na_2HPO_4 \cdot 6H_2O$ and $NaH_2PO_4 \cdot H_2O$ (MP Biomedicals, Germany). Water was purified by distillation in a Bi/Duplex distiller (Germany).(***I***) (Figure 1) CCDC 663194 and ***(II)*** were synthesized using the known method [15, 16].The structure and physicochemical data of ***(II)*** are described in the manuscript [17]. Complex***(II)*** according to the same synthetic route, elemental analysis, study of structure by methods of Mössbauer and EPR spectroscopy has a structure similar to the structure of complex ***(I),*** instead of only cysteamine thiol ligands are 2 molecules GSH [17].

Elemental analysis of ***(I)*** **and** ***(II)*** **polycrystals** were conducted at the Multi-access Analytic Centre IPCP RAS.

(***I***): $Fe_2S_3N_6C_4H_{19}O_{10\cdot5}$. Found, (%): C, 8.53; H, 2.77; N, 15.70; S, 17.71. Calculated, (%): C, 9.10; H, 3.60; Fe, 21.25; N, 15.93; O, 31.87; S, 18.27.

For ***(II)*** $Fe_2S_3N_{10}C_{20}H_{38}O_{17.}$ Found, %: Fe,11.40; C,24.52; H,3.91; N,14.28; O, 36.02; S, 9.79 %.Calculated, (%): Fe,11.45; C,24.54; H,3.89; N,14.31; O, 35.99; S, 9.82 %.

Operation technique in inert gas atmosphere [3].

Preparation of Hb solution. Homogenous solution of bovine Hb was prepared from commercial Hb product using the known method [18].

Decomposition of complexes ***(I)*** **or** ***(II)*** **at pH 7.0.** The experiments were carried out using the same original $6 \cdot 10^{-4}$ M solution of NIC. To the sample of NIC in a nitrogen-filled vessel was

added 0.05 M anaerobic Tris-HCl buffer pH 7.0 in order to obtain a NIC $6 \cdot 10^{-4}$ M solution, which was dissolved for 15 minutes and then frozen in liquid nitrogen in the shape of balls. For the purpose of experiments NIC was thawed under nitrogen flow for about 20 minutes until complete melting of the balls, and then solution aliquots of 0.75 ml were taken and inserted in a 4 ml anaerobic test cuvette (1 cm of optical path), containing 2.25 ml of 0.05 M anaerobic buffer pH 7.0 to achieve final NIC concentration of $1.5 \cdot 10^{-4}$ M. The reference cuvette contained 3 ml of buffer. The absorption spectra were recorded between 250-500 nm or 300-650 nm at appropriate time intervals at 25 °C.

Kinetics of *(I)* interaction with GSH. The experiments were carried out in nitrogen atmosphere. $6 \cdot 10^{-4}$ M ***(I)***solution prepared as described above was used for experiments and 10^{-2} M GSH solution in 0.1 M Tris-HCl buffer pH 7.0. 1.95 ml of anaerobic buffer and 0.75 ml of $6 \cdot 10^{-4}$ M ***(I)*** solution were inserted in a 4 ml anaerobic test cuvette with 1 cm optical path. The reaction was initiated by adding 0.3 ml of 10^{-2} M GSH solution. The final concentration of ***(I)*** in test cuvette was $1.5 \cdot 10^{-4}$ M. The reference cuvette contained anaerobic buffer pH 7.0 and***(I)*** of the same concentration as in the test cuvette. Further the difference absorption spectra were registered at appropriate intervals, as indicated in the Figures.

Kinetics of NIC (*(I)* or *(II)*) interaction with Hb. We used $6 \cdot 10^{-4}$ M solutions of either ***(I)*** or ***(II)*** in 0.05 M anaerobic Tris-HCl-buffer pH 7.0 after defrosting under nitrogen flow, prepared as described above. A 0.75 ml of NIC solution was transferred under nitrogen to an anaerobic test cuvette and a 4 ml comparison cuvette, containing such quantity of 0.05 M anaerobic buffer pH 7.0, so that the resulting volume of reaction solution after introduction of approx 0.11 ml of Hb $5.4 \cdot 10^{-4}$ M solution into test cuvette would be 3.0 ml. The reaction was initiated by adding Hb solution to the test cuvette to reach a $2 \cdot 10^{-5}$ M concentration. Final concentration of NIC solution in the test cuvette and reference cuvette was $1.5 \cdot 10^{-4}$ M. Further the difference absorption spectra were registered at appropriate intervals, as indicated in the figures. Similarly the interaction of Hb with NIC $1.5 \cdot 10^{-4}$ M in the presence of GSH 10^{-3} M in anaerobic Tris-HCl buffer pH 7.0 was studied. The buffer solution was inserted into anaerobic cuvettes (1.84 ml and 1.95 ml in the test and reference cuvette respectively), 0.75 ml NIC $6 \cdot 10^{-4}$ M and 0.3 ml of a 10^{-2} M GSH solution in 0.1 M Tris-HCl buffer pH 7.0. The reaction was initiated by adding the Hb solution in the test cuvette up to a $2 \cdot 10^{-5}$ M. Then the difference absorption spectra were registered at appropriate intervals, as indicated in the Figures.

Absorption spectra were recorded at 25 °C using a Specord M-40 spectrophotometer equipped with an interface for computer-aided registration of spectra and thermostatic cuvette holder.

Amount of Hb and HbNO was evaluated spectrophotometrically. For this purpose absorption spectra were factored by components as described in the paper [3].

Mass-spectrometric analysis was carried out using a 2020 Shimadzu LC-MS instrument that includes a liquid chromatograph LC-20 Prominence with matrix photo detector SPD-M20A (200-800 nm) and mass-selective quadrupole detector (m/z scanned mass range is 50-2000; ionization modes: DUIS/ESI/APCI). Analysis conditions: ionization method is electro spray ionization, ESI-MS, sample input method is direct input, solvent is acetonitril, incubation (25 °C), exposure mode is positive mode. Analysis sample was the reaction mixture of **(*I*)**with GSH at the end of reaction under nitrogen atmosphere in 0.005 M Tris-HCl-buffer pH 7. 2 ml vessels with a PTFE/Silicone/PTFE seal allowing samples to be inserted with a syringe, purged with nitrogen for about 10 minutes before the sample was inserted.

Results and discussion

1. **Decomposition of complexes *(I)*** and (***II).***

We studied decomposition of 2 NICs. (***I)*** (Figure 1) and its analog, NIC of the same structure as (***I)*** (Figure 1), but with GSH as the thiolate ligands, *bis*-(glutathione-2-thiolate) tetranitrosyl diiron (***II).*** We used 0.05M Tris-HCl buffer as a solvent, due to the simultaneous mass-spectrometric analysis of samples being conducted. In the phosphate buffer, where NICs had previously been dissolved [3], the phosphate spectrum superimposed the test sample's spectrum in the profile of multiple peaks. All investigations were conducted under a nitrogen atmosphere, as NO promptly interacts with O_2, producing nitrogen oxides with a rate constant of $2 \cdot 10^6$ $(M^{-1})^2$ s^{-1} at 25 °C [19]. Original NIC solution ($6 \cdot 10^{-4}$ M) was frozen to ensure an NIC solution of the same concentration is used. Figure 2 shows data concerning the change in the absorption spectrum of (***I)*** in solution, whereas Figure 3 (curve 3) shows the kinetics of NO evolution by the formation of HbNO. Hb demonstrates a specific absorption spectrum that alters as NO is attached. Therefore, as described in previous paper [3], for this class of NO donors, evolution of NO can be traced by the formation of HbNO. Since all NICs absorb in the visible spectrum, the experiment recorded differences in absorption spectra of the buffer and test system with Hb containing NIC in equal concentrations. The composition of reaction mixtures is described in the

Materials and methods section. By recording HbNO accumulation and fractioning of the absorption spectra into components, we measured the kinetics of HbNO formation (Figure 3). Using the following equation: $y(t) = y_o + A \cdot e^{-kt}$, we obtained the effective pseudo-first order rate constants (*k*) for this reaction (Table 1). The same investigation was carried out with (***II***) (Figures 4 and 3, curve 2). From Figure 3 follows that the rate of NO release from the complexes (***I***) and (***II***) are close in value. But, the comparison of Figures 2 and 4 (Table 1) shows that if the spectral changes in complex ***(I)*** occur within 8 hours, the spectral changes in (***II)*** continue up to 68 hours. This demonstrates the greater stability of the complex (***II).***

2. **Ligand exchange in *(I)* for GSH based on spectrophotometric data**

We have found that in an aqueous medium the reversible dissociation of ***(I)*** with the release of NO occurs [19]. Structural analog of ***(I)***, containing a penicillamine thiols instead of cysteamine**.** reversibly releases in an aqueous medium as NO, and penicillamine ligand **[**20]. So it was natural to expect that complex ***(I)*** could release its cysteamine thiol and exchange it for GS-. Therefore, in this paper, we investigated the interaction of (***I)*** with GSH.

In the reaction medium containing ***(I)*** and GSH (Figure 5) the absorption spectrum, the parameters of which match the absorption spectra of ***(II)*** (Figure 4), grew. The maximum is gradually changed from 320 nm (spectrum 1) to 315 nm (spectra 14-26) as in ***(II)***. Gradually appears the second maximum at 362 nm, which is close to the second maximum of spectrum (***II)*** (365 nm). The increase of maximum absorption took place up to 68 h. At the same time, the concentration of the resulting (***II)*** (taking into account that of (***II)*** at 315 nm is equal to $8.18 \cdot 10^3$ $M^{-1}cm^{-1}$, Figure 4) was $1.16 \cdot 10^{-4}$ M while the concentration of the original (***I)*** was $1.5 \cdot 10^{-4}$ M; i.e. the output was 77 %. Output cannot reach 100% because the (***II***) decay takes place in parallel. Apparently observed in this work the exchange of thiolate ligands depends on the bond strength of thiolate ligands with Fe. In the system (***I)***-GSH and when Hb was present in the (***I)***-GSH system, HbNO accumulated with *k* equal $5 \cdot 10^{-6}$ s^{-1} , very slowly. Thus in (***I)***-GSH system, accompanied by the formation of (***II***), these NICs become more prolonged donor NO. It is also important for their metabolism.

Table 1. Results of kinetic experiments

Figures number	NIC	Process	k^*, s^{-1}

2	***(I)***	Decomposition	$(6 \pm 0.6)\cdot 10^{-5}$
4	***(II)***	Decomposition	$(3.8. \pm 0.4)\cdot 10^{-5}$
5	***(I)***	Interaction with GSH	$(5 \pm 0.5)\cdot 10^{-6}$
3	***(I)***	Interaction with Hb	$(2.5 \pm 0.2)\cdot 10^{-5}$
3	***(II)***	Interaction with Hb	$(2.6 \pm 0.3)\cdot 10^{-5}$
3	***(I)***	Interaction with GSH and Hb	$(5 \pm 0.5)\cdot 10^{-6}$

k^* are the effective pseudo-first order rate constants.

2. Mass spectrometry analysis

Mass spectral analysis of the mixture of (***I)*** with GSH (Figure 5) was performed (figure 6). In the course of analyzing products of the interaction of (***I)*** with GSH after 68 h-incubation at 25 °C, which corresponded to maximum output of the product of the interaction of these compounds (Figure 5), the cation of the ***(II)*** was detected (Table 2). Moreover the spectrum shows a certain amount of the split GSH thiolate ligand and product of its oxidized form GS-SG and also dithiol, cysteamine-GS . Thus, the results of mass-spectral experiments of the water solutions of the reaction system (Figure 6) qualitatively correspond to the data obtained in the spectrophotometric study.

Table 2. The results of mass spectrometry (Figure 6)

Ion mass singly charged), m/z	Ion type	Formula for M, subunit or sequence	Origin and other comments
308.5	$[M + H]^+$	GSH	Glutathione, $C_{10}O_6N_3SH_{17}$
383.1	$[M + H]^+$	CysAm*-SG	Product of interaction of GSH with CysAm
613.2	$[M + H]^+$	GS-SG	Oxidized form of glutathione
635	$[M + Na]^+$	GS-SG	Oxidized form of glutathione

845	$[M + H]^+$	$Fe_2(GSH)_2(NO)_4$	Cation of (***II***)

*CysAm is cysteamine

Conclusions

This paper firmly shows for the first time that NIC bearing a thiolate ligands, cysteamine $\{Fe_2[S(CH_2)_2NH_3]_2(NO)_4\}SO_4 \cdot 2.5H_2O$ (***I***) in aqueous medium in the presence of GSH after removing their thiolate ligands, replaces them with GS-, thus forming another NIC with 2 GS^- ligands (***II***), which is quite decomposition-resistant as seen from our experiment. We assume this may influence the important role of (***I***) in biotransformations, connected with anti-tumor activity. GSH is a tripeptide and is bonded with Fe in (***II***) by the S-group of cysteine, which is located between glutamic acid and glycine. These two amino acids likely "shield" the Fe-S bond in (***II***) from attack by thiols and water. In (***I***)-GSH system, accompanied by the formation of (***II***), these NICs are more prolonged donor NO. It is also important for their metabolism.

Supplementary information..

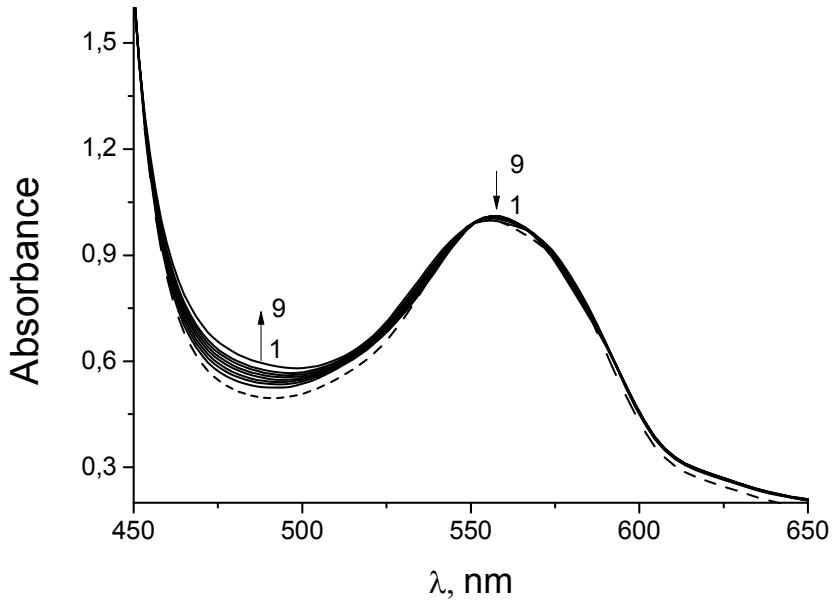

8

Figure a) Kinetics of change of difference spectra at the interaction of $1.5 \cdot 10^{-4}$ M (***I***) with 10^{-3} M GSH in $2 \cdot 10^{-5}$ M Hb presence in 0.05 M Tris-HCl buffer pH 7.0 at 25 ^{0}C . Dotted line (1) is spectrum of Hb. Spectra 2-5 were registered at 0.08 (2), 0.33 (3), 0.6 (4) h after start of reaction; spectra 5-13 were registered with intervals 1 h , spectrum 15 at h after start of reaction. Conditions of reaction: 25^{o}C, solvent is 0.05 M Tris-HCl buffer, pH 7.

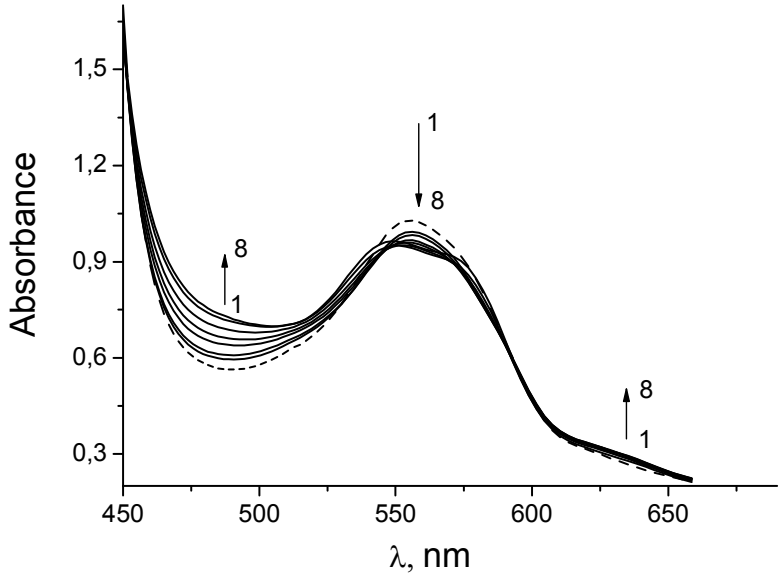

Figure b) Kinetics of change of difference spectra at the interaction of ***(II)*** ($1.5 \cdot 10^{-4}$ M) with Hb ($2 \cdot 10^{-5}$ M). Dotted line (1) is spectrum of Hb. Spectra 2-8 were registered at 0.5 (2), 1 (3), 3 (4), 5 (5), 7 (6), 9 (7), 11(8) h after start of reaction. Conditions of reaction: 25 ^{o}C, solvent is 0.05 M Tris-HCl buffer, pH 7.0

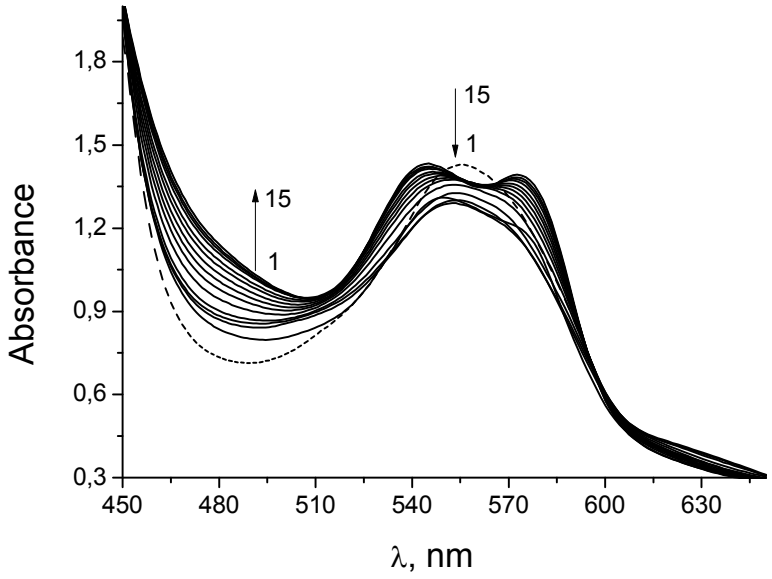

Figure c) Kinetics of change of difference spectra at the interaction of (***I***) ($1.5 \cdot 10^{-4}$ M) with Hb ($2 \cdot 10^{-5}$ M). Dotted line (1) is spectrum of Hb. Spectra 2-5 were registered at 0.08 (2), 0.33 (3), 0.6 (4) h after start of reaction; spectra 5-13 were registered with intervals 1 h , spectrum 15 at 11 h after start of reaction. Conditions of reaction: 25 °C, solvent is 0.05 M Tris-HCl buffer, pH 7.0.

Acknowledgments

This study was financially supported by the RFBR (Grant No. 13-03-00549).

We wish to thank Dr. A.V. Chudinov for the preparation of program of computer processing of absorption spectra by the least square method using program MathCaD and O.K. Kononykhina for help in work.

Notes and references.

1. N. A. Sanina, S. M. Aldoshin, *Russ. Chem. Bull., Int. Ed*., 2004, **53**, 2428.

2. J. L. Bourassa, P. C. Ford, *Coord. Chem. Rev*., 2000, **200**, 887.

3. N. A. Sanina, L. A. Syrtsova, N. I. Shkondina, T. N. Roudneva, E. S. Malkova, T. A. Bazanov, A. I. Kotelnikov, S. M. Aldoshin, *Nitric Oxide: Biol.&Chem*., 2007, **16**, 181.

4. N. A. Sanina, T. N. Roudneva, I. V. Sulimenkov, N. P. Konovalova, T. E. Sashenkova, S. M. Aldoshin, *Ross. Khim. Zhurn*., 2009, **LIII**, 164.

5. N. A. Sanina, O. S. Zhukova, S. M. Aldoshin, N. S. Emel'janova, G. K. Gerasimova, Use of tetranitrosyl complex with thiophenol as anti-tumor drag, *Patent RU N° 242924*, 2011.

6. H. Prast, A. Philippu, *Prog. Neurob*., 2001, **64**, 51.

7. E. T. Yukl, M. A. Elbaz, M. M. Nakano, P. Moenne-Loccoz, *Biochemistry*, 2008, **47**, 13084.

8. J. C. Drapier, C. Pellat, Y. Henry, *J. Biol. Chem*., 1991, **266**, 10162.

9. C. Bogdan, *Nat. Immunol*., 2001, **2**, 907.

10. L. J. Ignarro, G. M. Buga, K. S. Wood, R. E. Byrns, G. Chaudhuri, *Proc. Natl. Acad. Sci. USA*, 1987, **84**, 9265.

11. N. A. Sanina, L. I. Serebryakova, N. S. Shul'zhenko, O. I. Pisarenko, T. N. Roudeva, S. M. Aldoshin, Application of binuclear sulphur-nitrosyl complex of anion type iron as vasodepressor medication, 2437667 C1, 2011.

12. N. A. Sanina, O. S. Zhukova, Z. S. Smirnova, L. M. Borisova, M. P. Kiseleva, S. M. Aldoshin*, Russ. J. Biotherapeut*., 2008, **1**, 52.

13. D. M. Townsend, K. D. Tew, H. Tapiero, *Biomedicine & Pharmacotherapy*, 2003, **57**,145.

14. P. M. Chumakov, *Biochemistry (Moscow)*, 2007, **72**, 1399.

15. T. N. Roudneva, N. A. Sanina, K. A. Lyssenko, S. M. Aldoshin, M. Yu. Antipin, N. S. Ovanesyan,*Mendeleev Communication*, 2009, **19**, 253. CCDC 663194 complex ***(I)*** $[Fe_2(S(CH_2)_2NH_3)_2(NO)_4]SO_4 \cdot 2.5H_2O$ contains the supplementary crystallographic data for this paper. These data can be obtained free of charge from Cambridge Crystallographic Data Centre *via* www.ccdc.cam.ac.uk/data_request/cif.

16. N. A. Sanina, K. A. Lysenko, O. S. Zhukova, T. N. Rudneva, N. S. Emel'janova, S. M. Aldoshin, Water soluble binuclear cation nitrosyl iron complexes with natural aliphatic thiolyls processing cytotoxic, apoptotic and NO-donor activity, *Patent RU N° 2441873 C2*, 2006.

17. N. A. Sanina, New class of nitric monoxide donors: structure and properties of nitrosyl iron complexes with functional sulphur containing ligands: doctoral dissertation, Institute of Problems of Chemical Physics, Chernogolovka, 2011.

Reference [17] can be seen in Internet: a) http://www.dissercat.com/content/novyi-klass-donorov-monooksida-azota-stroenie-i-svoistva-nitrozilnykh-kompleksov-zheleza-s-f;
b) http://test.vak.ed.gov.ru/common//img/uploaded/files/SaninaNA.doc

c) http://govrudocs.ru/navigate/300/index-563867.html

18. N. A. Sanina, L. A. Syrtsova, N. I. Shkondina, E. S. Malkova, A. I. Kotelnikov, S. M. Aldoshin. *Russ. Chem. Bull., Int. Ed*., 2007, **56**, 761.

19. A. M. Miles, D. A. Wink, J. C. Cook, M. B. Grisham In: L.Packer (Ed.) *Methods in Enzymology*. Determination of nitric oxide using fluorescence spectroscopy. Academic Press, 1996, **268,** Part A, 105

20. O. V. Pokidova, L. A. Syrtsova, N. A. Sanina, B. L. Psikha. N. I. Shkondina, T. N. Rudneva, A. I. Kotelnikov, *Proceedings of the XXI International Conference and Discussion Club "New Information Technologies in Mrdicine, Biology, Pharmacology and Ecology*". Ukraine, Crimea, Yalta-Gursuf, 5-15 June 2013, p. 156-157. Reference [20] can be seen in Internet: http://www.glorioz.com

Figures

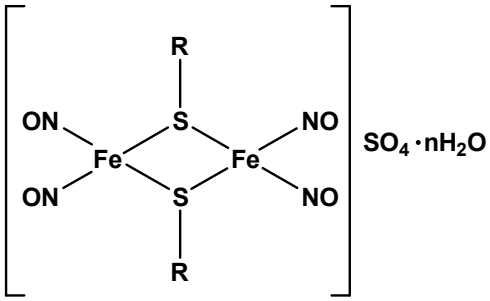

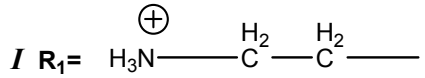

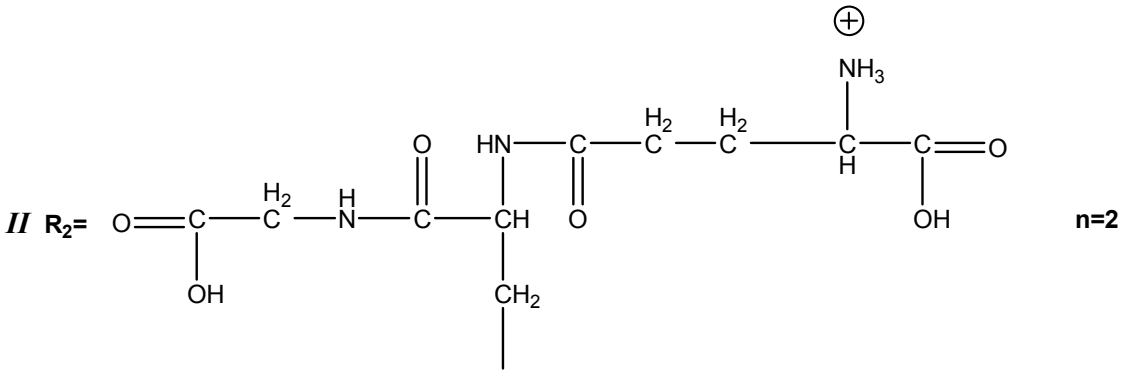

Figure 1 Chemical structures of the tetranitrosyl iron complexes ***(I)*** and ***(II)***

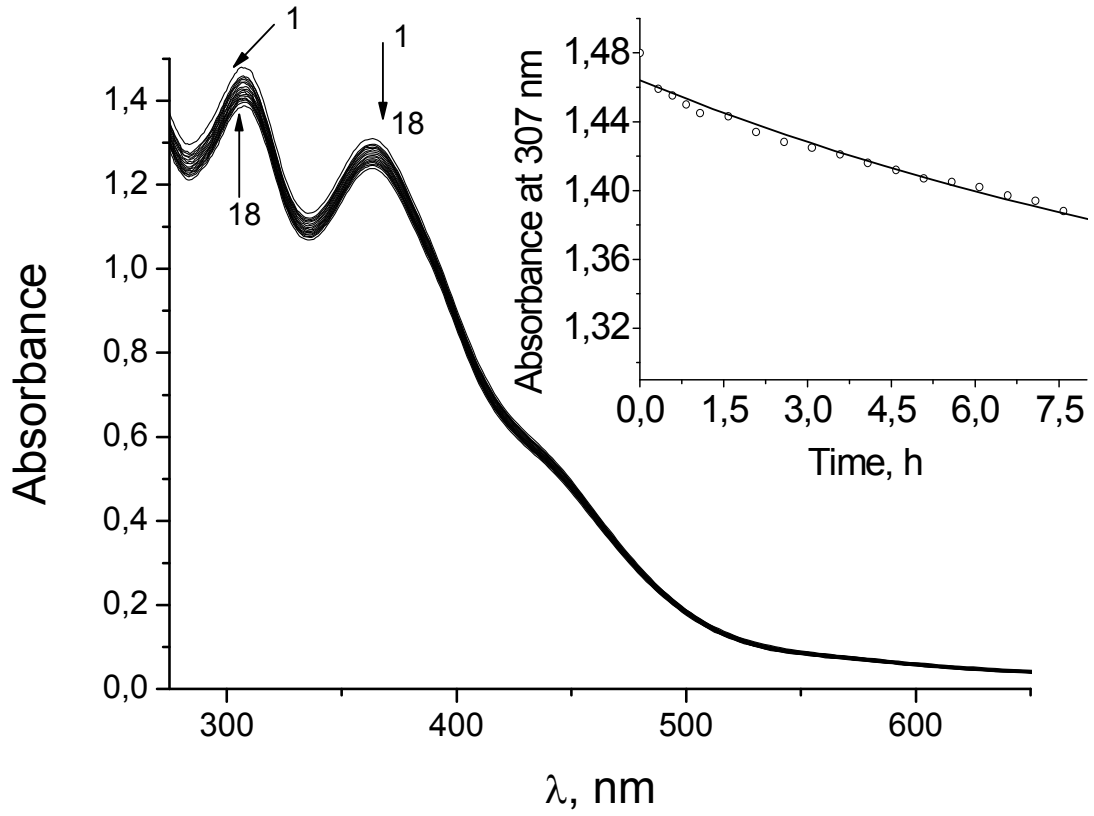

Figure 2 Kinetics of change of absorption spectrum of $1.5 \cdot 10^{-4}$ M (***I***) in 0.05 M Tris-HCl buffer pH 7.0 at25 ^{0}C: spectrum (1) was registered at 30 s, spectra 2-5 further were registered with intervals 15 min, spectra 6-18 were registered with intervals 30 min, spectrum 18 at 8 h after start of reaction. Spectra 1-18 have 2 maximum: λ_1 = 307 нм и λ_2 = 363 нм. The inset shows kinetics of (***I***) ($1.5 \cdot 10^{-4}$ M) decomposition in 0.05 M Tris-HCl-buffer pH 7.0 at 25 ^{0}C (for the experimental data shown in Figure). Circles are experimental data. Approximation (theoretical curve) was made by means of equation: $y(t) = y_o + A \cdot e^{-kt}$. ***(I)*** is complex $\{Fe_2[S(CH_2)_2NH_3]_2(NO)_4\}SO_4 \cdot 2.5H_2O$.

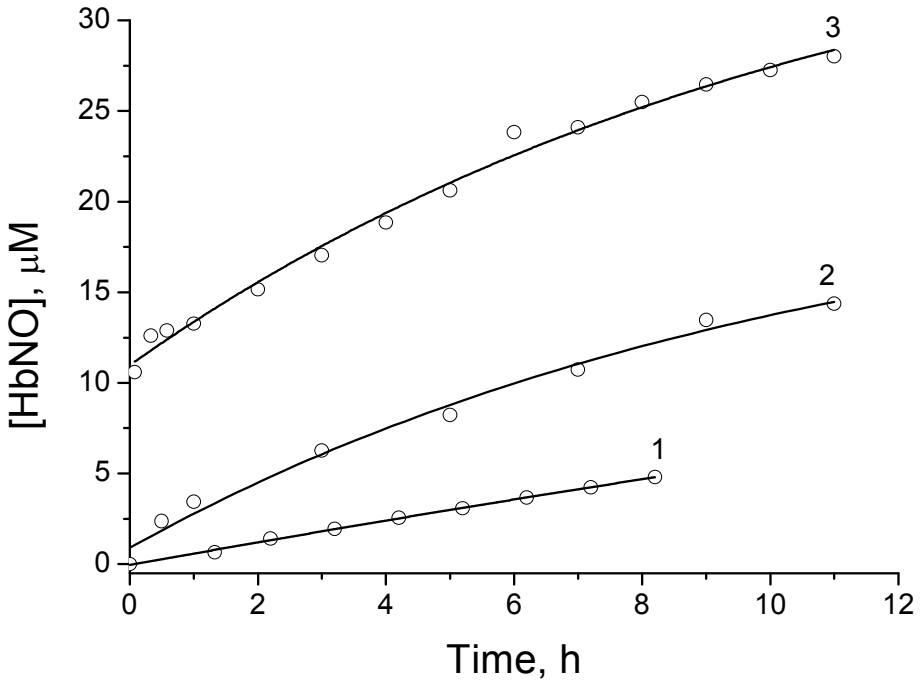

Figure 3 1) Kinetics of HbNO formation at interaction of ***(I)*** with GSH in Hb presence on the base of the experimental data shown in Figure a). Circles are the experimental data. Solid line is the approximation by means of equation $y(t) = y_o + A\cdot(1 - e^{-kt})$. . 2) Kinetics of HbNO formation at interaction of ***(II)*** with Hb on the base of the experimental data shown in Figure b. Circles are the experimental data. Solid line is the approximation by means of equation: $y(t) = y_o + A\cdot(1 - e^{-kt})$. ***(I)*** is $\{Fe_2[S(CH_2)_2NH_3]_2(NO)_4\}SO_4\cdot 2.5H_2O$, ***(II)*** is complex $[Fe_2(SC_{10}H_{17}N_3O_6)_2(NO)_4]SO_4\cdot 2H_2O$. 3) Kinetics of HbNO formation at interaction of (***I***) with Hb on the base of the experimental data shown in Figure c). Circles are the experimental data. Solid line is the approximation by means of equation: $y(t) = y_o + A\cdot(1 - e^{-kt})$.. (***I***) is $\{Fe_2[S(CH_2)_2NH_3]_2(NO)_4\}SO_4\cdot 2.5H_2O$. (Figures a, b, c are in **Supplementary Data**).

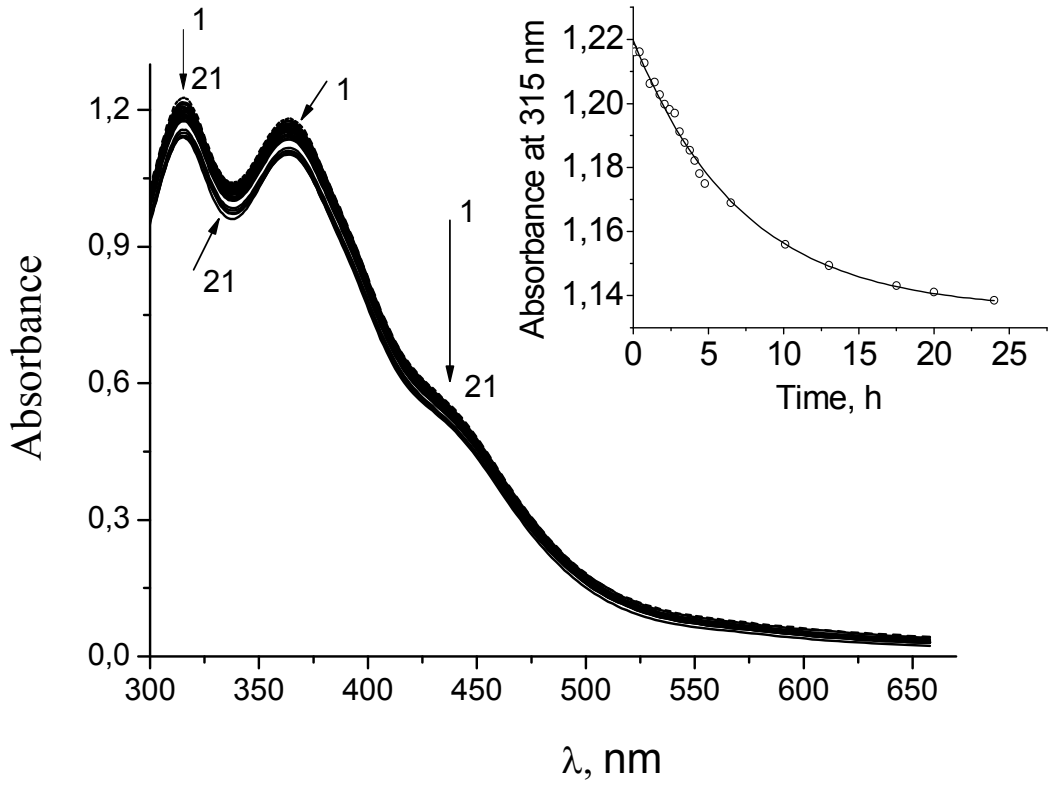

Figure 4 Kinetics of change of absorption spectrum of (***II***) ($1.5 \cdot 10^{-4}$ M): spectra were registered at 30 s (1), 5 (2) min after start of reaction. Spectra 3-16 were registered further with intervals 20 min. Spectra 17-22 were registered at 6.5 (17), 10.1 (18), 13 (19), 17.5 (20), 20 (21), 24 (22) h after start of reaction. Conditions of reaction: 25 °C, solvent is 0.05 M Tris-HCl buffer, pH 7.0. Spectra 1-22 have 2 maximum: λ_1 = 315 nm and λ_2 = 365 nm; $_{315\ nm}$ is equal to $8.2 \cdot 10^3$ $M^{-1} \cdot см^{-1}$. The inset shows kinetics of (***II***) ($1.5 \cdot 10^{-4}$ M) decomposition in 0.05 M Tris-HCl-buffer pH 7.0 at 25 ^{0}C (for the experimental data shown in Figure). Circles are experimental data. Approximation (theoretical curve) was made by means of equation: $y(t) = y_o + A \cdot e^{-kt}$. (***II***) is complex $[Fe_2(SC_{10}H_{17}N_3O_6)_2(NO)_4]SO_4 \cdot 2H_2O$

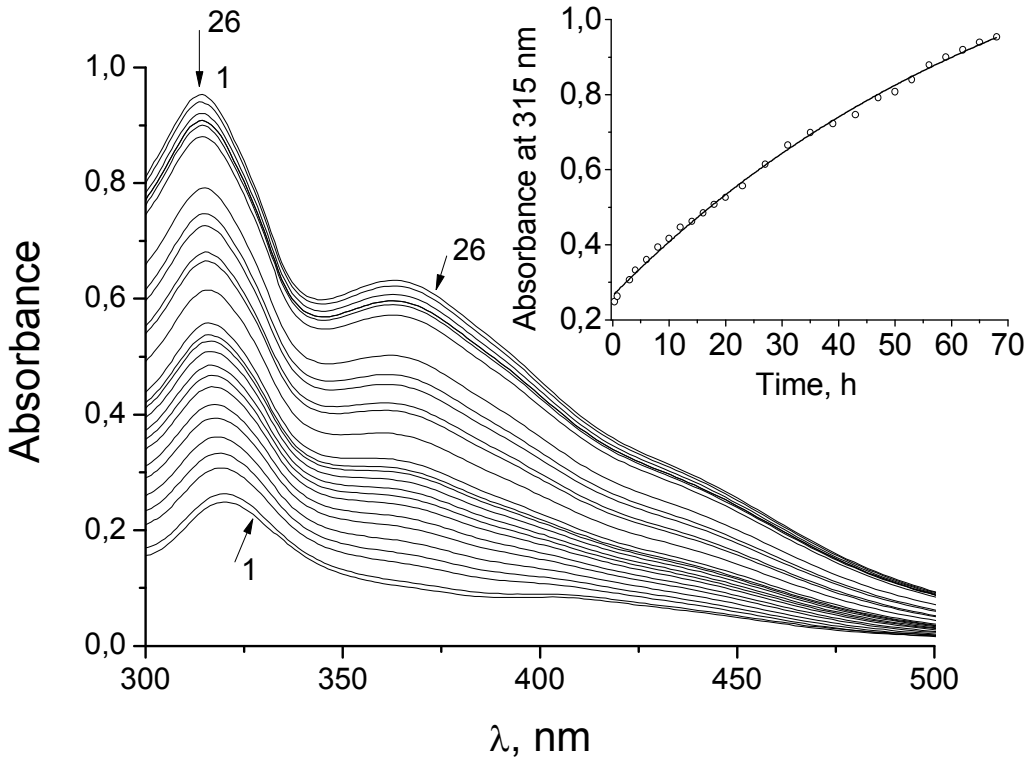

Figure 5 Kinetics of change of absorption spectrum at interaction of ***(I)*** ($1.5 \cdot 10^{-4}$ M) with GSH (10^{-3} M): spectra were registered at 20 min (1), 50 min (2). 3 h (3) after start of reaction. Spectra 4-12 were registered further with interval 1 h. Then spectrum 13 through 3 h after spectrum 12. Spectra 14-19 were registered with interval 4 h, spectra 20-26 with interval 3 h, spectrum 26 at 68 h after start of reaction. Conditions of reaction: 25°c, solvent is 0.05 M Tris-HCl buffer, pH 7.0. Spectra 15-26 have 2 maximum: λ_1 = 315 nm and λ_2 = 362 nm. . The inset shows kinetics of ***(II)*** accumulation at interaction of ***(I)*** with GSH on the base of the experimental data shown in Figure. Circles are the experimental data. Approximation (theoretical curve) was made by means of equation $y(t) = y_o + A \cdot e^{-kt}$. ***(II)*** is complex $[Fe_2(SC_{10}H_{17}N_3O_6)_2(NO)_4]SO_4 \cdot 2H_2O$.

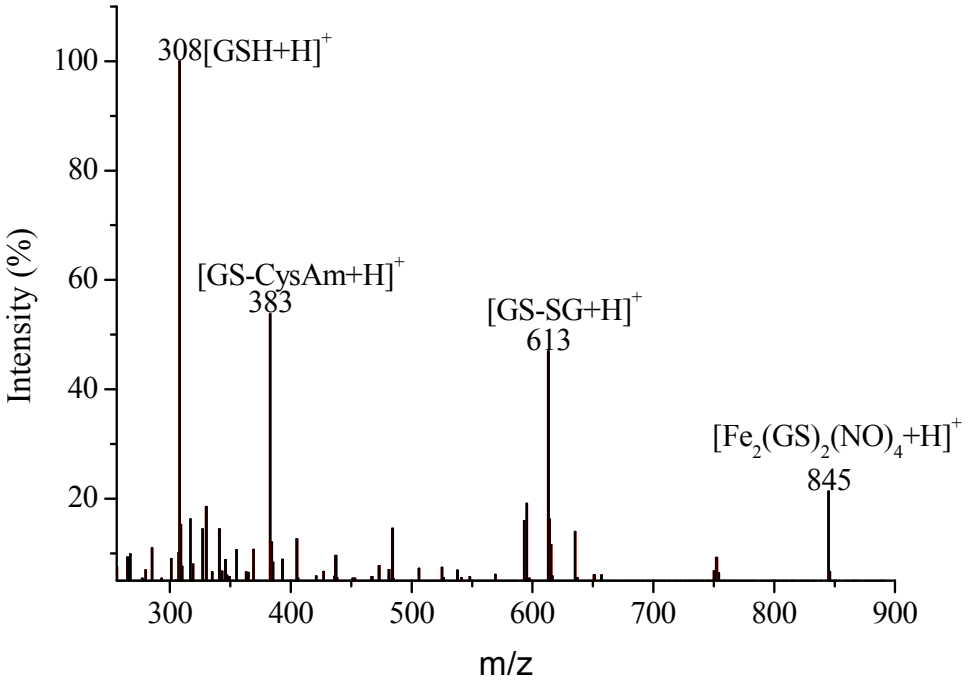

Figure 6 Mass spectrum (ESI, +4.5 kV) of the mixture of $1.5 \cdot 10^{-5}$ M ***(I)*** and 10^{-4} M GSH (as in experiment, shown on Figure 5, after dilution with water 10 times) after 68 h from the start of the reaction. Solvent is 0.005 M Tris-HCl-buffer, pH 7.0. ***(II)*** is complex $[Fe_2(SC_{10}H_{17}N_3O_6)_2(NO)_4]SO_4 \cdot 2H_2O$, GSH – glutathione, GS-SG - oxidized glutathione, CysAm - цистеамин, $Fe_2(GS)_2(NO)_4$ is cation of the complex (***II***).

Figures legends

Figure 1 Chemical structures of the tetranitrosyl iron complexes ***(I)*** and ***(II .)***

Figure 2 Kinetics of change of absorption spectrum of $1.5 \cdot 10^{-4}$ M (***I***) in 0.05 M Tris-HCl buffer pH 7.0 at25 ^{0}C: spectrum (1) was registered at 30 s, spectra 2-5 further were registered with intervals 15 min, spectra 6-18 were registered with intervals 30 min, spectrum 18 at 8 h after

start of reaction. Spectra 1-18 have 2 maximum: λ_1 = 307 нм и λ_2 = 363 нм. The inset shows kinetics of (***I***) ($1.5 \cdot 10^{-4}$ M) decomposition in 0.05 M Tris-HCl-buffer pH 7.0 at 25 ^{0}C (for the experimental data shown in Figure). Circles are experimental data. Approximation (theoretical curve) was made by means of equation: $y(t) = y_o + A \cdot e^{-kt}$. ***(I)*** is complex $\{Fe_2[S(CH_2)_2NH_3]_2(NO)_4\}SO_4 \cdot 2.5H_2O$.

Figure 3 1) Kinetics of HbNO formation at interaction of ***(I)*** with GSH in Hb presence on the base of the experimental data shown in Figure a). Circles are the experimental data. Solid line is the approximation by means of equation $y(t) = y_o + A \cdot (1 - e^{-kt})$. . 2) Kinetics of HbNO formation at interaction of ***(II)*** with Hb on the base of the experimental data shown in Figure b. Circles are the experimental data. Solid line is the approximation by means of equation: $y(t) = y_o + A \cdot (1 - e^{-kt})$. ***(I)*** is $\{Fe_2[S(CH_2)_2NH_3]_2(NO)_4\}SO_4 \cdot 2.5H_2O$, ***(II)*** is complex $[Fe_2(SC_{10}H_{17}N_3O_6)_2(NO)_4]SO_4 \cdot 2H_2O$. 3) Kinetics of HbNO formation at interaction of (***I***) with Hb on the base of the experimental data shown in Figure c). Circles are the experimental data. Solid line is the approximation by means of equation: $y(t) = y_o + A \cdot (1 - e^{-kt})$. (***I***) is $\{Fe_2[S(CH_2)_2NH_3]_2(NO)_4\}SO_4 \cdot 2.5H_2O$. (Figures a, b, c are in **Supplementary Data**).

Figure 4. Kinetics of change of absorption spectrum of (***II)*** ($1.5 \cdot 10^{-4}$ M): spectra were registered at 30 s (1), 5 (2) min after start of reaction. Spectra 3-16 were registered further with intervals 20 min. Spectra 17-22 were registered at 6.5 (17), 10.1 (18), 13 (19), 17.5 (20), 20 (21), 24 (22) h after start of reaction. Conditions of reaction: 25 ^{o}C, solvent is 0.05 M Tris-HCl buffer, pH 7.0. Spectra 1-22 have 2 maximum: λ_1 = 315 nm and λ_2 = 365 nm; $_{315\,nm}$ is equal to $8.2 \cdot 10^3$ $M^{-1} \cdot см^{-1}$. The inset shows kinetics of (***II)*** ($1.5 \cdot 10^{-4}$ M) decomposition in 0.05 M Tris-HCl-buffer pH 7.0 at 25 ^{0}C (for the experimental data shown in Figure). Circles are experimental data. Approximation (theoretical curve) was made by means of equation: $y(t) = y_o + A \cdot e^{-kt}$. ***(II)*** is complex $[Fe_2(SC_{10}H_{17}N_3O_6)_2(NO)_4]SO_4 \cdot 2H_2O$

Figure 5 Kinetics of change of absorption spectrum at interaction of ***(I)*** ($1.5 \cdot 10^{-4}$ M) with GSH (10^{-3} M): spectra were registered at 20 min (1), 50 min (2). 3 h (3) after start of reaction. Spectra 4-12 were registered further with interval 1 h. Then spectrum 13 through 3 h after spectrum 12. Spectra 14-19 were registered with interval 4 h, spectra 20-26 with interval 3 h, spectrum 26 at 68 h after start of reaction. Conditions of reaction: 25^{o}c, solvent is 0.05 M Tris-HCl buffer, pH 7.0. Spectra 15-26 have 2 maximum: λ_1 = 315 nm and λ_2 = 362 nm. . The inset shows kinetics of ***(II)*** accumulation at interaction of ***(I)*** with GSH on the base of the experimental data shown

in Figure. Circles are the experimental data. Approximation (theoretical curve) was made by means of equation $y(t) = y_o + A \cdot e^{-kt}$. ***(II)*** is complex $[Fe_2(SC_{10}H_{17}N_3O_6)_2(NO)_4]SO_4 \cdot 2H_2O$.

Figure 6. Mass spectrum (ESI, +4.5 kV) of the mixture of $1.5 \cdot 10^{-5}$ M ***(I)*** and 10^{-4} M GSH (as in experiment, shown on Figure 5, after dilution with water 10 times) after 68 h from the start of the reaction. Solvent is 0.005 M Tris-HCl-buffer, pH 7.0. ***(II)*** is complex $[Fe_2(SC_{10}H_{17}N_3O_6)_2(NO)_4]SO_4 \cdot 2H_2O$, GSH – glutathione, GS-SG - oxidized glutathione, CysAm - цистеамин, $Fe_2(GS)_2(NO)_4$ is cation of the complex (***II***).